JOURNAL OF CATALYSIS **163,** 501–505 (1996)
ARTICLE NO. 0353

NOTE

Crystalline, Microporous Zirconium Silicates with MEL Structure

The isomorphous substitution of Si^{4+} by Ti^{4+} and Sn^{4+} in the silicalite-2 (ZSM-11, MEL) framework has been the subject of some recent reports (1–3). The possibility of substituting silicon by zirconium in the framework of ZSM-5 (MFI) by hydrothermal synthesis has been reported but not really substantiated by experimental evidence (4–8). In our earlier attempts, based on the unit cell volume expansion of about 21 $Å^3$ of the MFI structure, it was presumed that only 0.6 Zr atom per unit cell of MFI could be incorporated (9). In this communication, we report for the first time the synthesis of crystalline and microporous Al-free zirconium silicates with MEL structure. The presence of zirconium in the MEL framework is elucidated by X-ray diffraction (XRD), framework FTIR spectroscopy, diffuse reflectance UV-visible (DR UV-Vis) spectroscopy, and catalytic activity in the hydroxylation of phenol, using hydrogen peroxide as oxidant. The acid sites of all samples are determined by pyridine adsorption studies.

The hydrothermal synthesis of Zr-silicates was carried out using the following molar composition of the gel: 1.0 SiO_2 : x ZrO_2 : 0.4 TBAOH : 30 H_2O, where x = 0.0033 to 0.015. In a typical synthesis, a solution of 25.95 g of tetrabutylammonium hydroxide (TBAOH) (Aldrich, 40% aqueous) was added dropwise to 21.25 g of tetraethyl orthosilicate (TEOS) (Aldrich, 98%). This mixture was stirred for 30 min at 298 K in order to complete the hydrolysis of TEOS. To the above mixture, a solution of 0.24 g of zirconium tetrachloride ($ZrCl_4$) (Merck, 99%) in 5 g of distilled water was added slowly. The resulting mixture was stirred for about 1 h to get a homogeneous solution. Finally, the remaining volume of water was added and after stirring for 30 min, the liquid gel (pH = 12.20) was transferred to a stainless steel autoclave. The crystallization was conducted at 443 K for three days, under static condition. After the crystallization, the solid product was filtered, washed with deionized water, dried at 383 K, and calcined in air at 823 K for 16 h. The product yield was 80 wt%. Four such samples having different Si/Zr ratios (65 to 300) were prepared. All the zirconium silicate (Zr-Sil-2) samples were treated with 1 *M* ammonium acetate solution to remove alkali metal impurities, if any and then further calcined at 773 K in air for 8 h. For comparison, a silicalite-2 (silica polymorph with MEL structure) (Sil-2) sample and a Zr-impregnated silicalite-2 sample were prepared. The latter was made by impregnating Sil-2 with an aqueous solution of $ZrCl_4$ and then calcining at 773 K. An amorphous Zr-silica sample (Si/Zr = 100) was also prepared from the precursor gel solution which was not subjected to autoclaving and crystallization.

The samples were characterized by XRD (Rigaku, D-MAX III VC model, with Ni filtered Cu$K\alpha$ radiation), SEM (Leica Stereoscan 440 model), framework IR spectroscopy (Nicolet, 60 SXB model) and DR UV-visible spectroscopy (Shimadzu, UV-VIS spectrophotometer 2101 PC model). The *in situ* IR spectra of adsorbed pyridine were recorded (resolution 2 cm^{-1}) on a Digilab FTS-60 spectrometer after evacuation of the self-supported Zr-silicate samples at 773 K for 16 h, adsorption of pyridine at room temperature, and subsequent evacuation at 348–473 K. The elemental analysis was performed using an ICP spectrometer (John Yvon-JY-38 VHR) and the energy dispersive X-ray analysis (EDX) with a Kevex attachment to the SEM. The micropore areas and micropore volumes were calculated from the N_2 adsorption isotherms at liquid N_2 temperature (Coulter 100CX Omnisorb). The monolayer volumes were taken at $p/p_o = 0.05$, where all the micropores are filled up. The mesopore areas were obtained from the *t*-plots of N_2 adsorption data at higher partial pressures. The amounts of water, *n*-hexane, and cyclohexane adsorbed by the calcined samples were measured gravimetrically at a fixed $p/p_o = 0.5$ at 293 K on a Cahn (2000 G) electrobalance. The samples were evacuated at 673 K for 5 h prior to adsorption.

The hydroxylation of phenol was carried out using aqueous H_2O_2 (30 wt%) as oxidant. In a standard run, 5 g of phenol, 10 g of water, and 0.5 g of catalyst were taken in a 50 mL reactor and heated to 353 K in an oil bath. Next 2.13 g of H_2O_2 (phenol/H_2O_2 mole ratio = 3) was added to the reaction mixture and the reaction was continued for 10 h. The products were analyzed by GC (HP, 5880A) equipped with a 50-m long methyl-silicon gum capillary column and flame ionization detector.

The XRD profiles of the calcined Zr-Sil-2 samples (Fig. 1A) are similar to that of Sil-2 (10) and exhibit a high crystallinity, without any impurity phase. The interplanar *d* spacings of Sil-2 shift to higher values due to the incorporation of the larger zirconium ions (Shannon ionic radii: $Si^{4+} = 0.26$ and $Zr^{4+} = 0.59$ Å). The unit cell parameters

0021-9517/96 $18.00

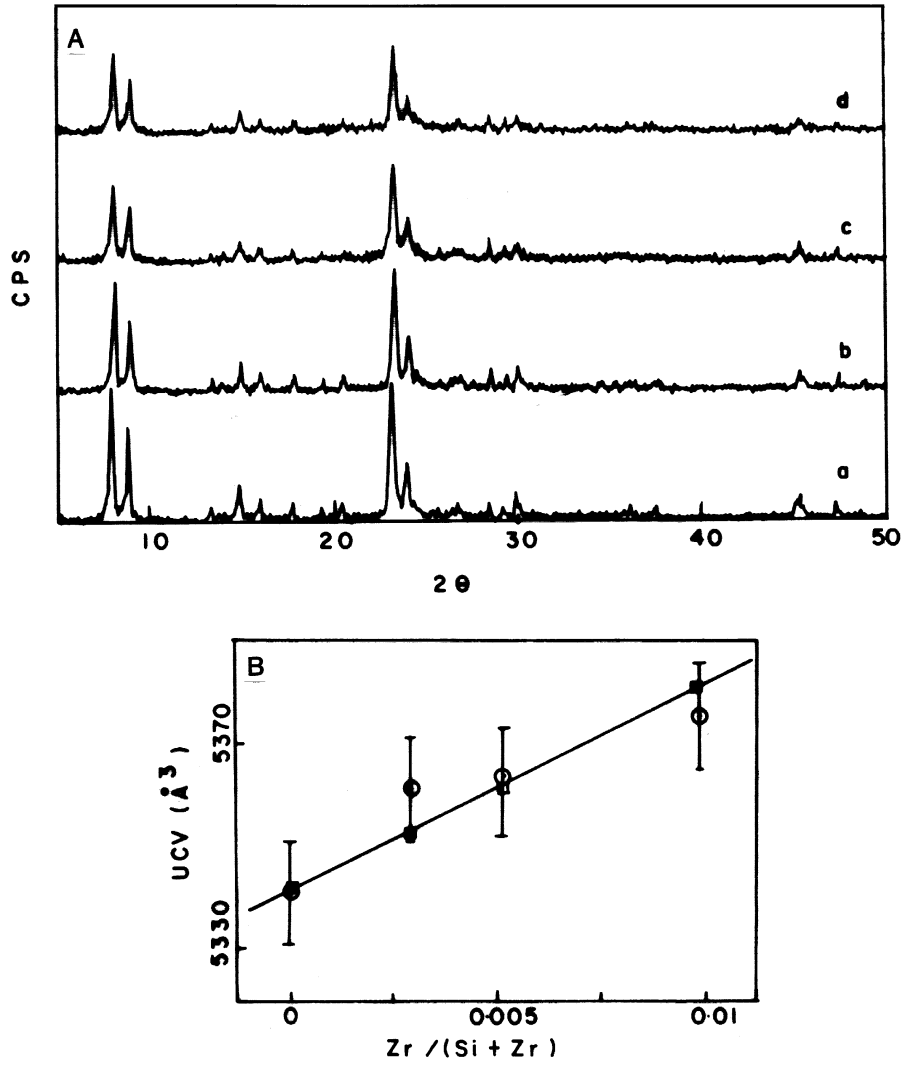

FIG. 1. (A) X-ray diffraction profiles of calcined silicalite-2 (MEL) sample (curve a) and Zr-Sil-2 samples prepared by hydrothermal synthesis with Si/Zr molar ratios of 300, 200, and 100 (curves b to d, respectively). (B) Increase in unit cell volume (Experimental (○) Theoretical (□)) with Zr content in the samples.

were refined by least-squares fitting. Although the fitting makes use of selected reflections only, yet a reasonable standard deviation and a correlation coefficient (~0.91) are obtained. The unit cell volume (UCV) is found to increase linearly as a function of zirconium content (Fig. 1B). It is reasonable to consider that this expansion in UCV corresponds to isomorphous substitution of zirconium in the silicalite framework. Figure 1B compares the experimental UCV with that calculated assuming replacement of Si^{4+} by Zr^{4+} in tetrahedral positions. A very good agreement between the two, within the experimental errors (shown by error bars) up to a metal concentation (x) of 0.01 (Si/Zr = 100) is observed. For preparations where $x > 0.01$, there was no clear gel formation and the excess zirconium precipitated as ZrO_2. SEM confirms the absence of any amorphous material around Zr silicate crystals. The particle size of pure silicalite sample is about 6 μm while Zr-Sil-2 samples showed 1.5–2.0 μm cuboid crystals in the form of spherical aggregates (Fig. 2).

The framework FTIR spectrum of Zr Sil-2 (Fig. 3, curve a) indicates a shoulder (sh) at about 960 cm^{-1} which may be attributed to Si–O–Zr asymmetric stretching vibrations (V_{as}), from the possible substitution of zirconium in the Si–O–Si linkages. However, no such absorption was observed in Zr-impregnated Sil-2 and Zr-amorphous silica samples (curves b and c, respectively). A similar band near 960 cm^{-1} has been reported for the Si–O–Ti linkages in SiO_2/TiO_2 and Ti substituted zeolites (TS-1 and TS-2) (11–15). For well-dispersed zirconia on silica, Dang *et al.* (16) have observed a band at 945 cm^{-1} from difference IR

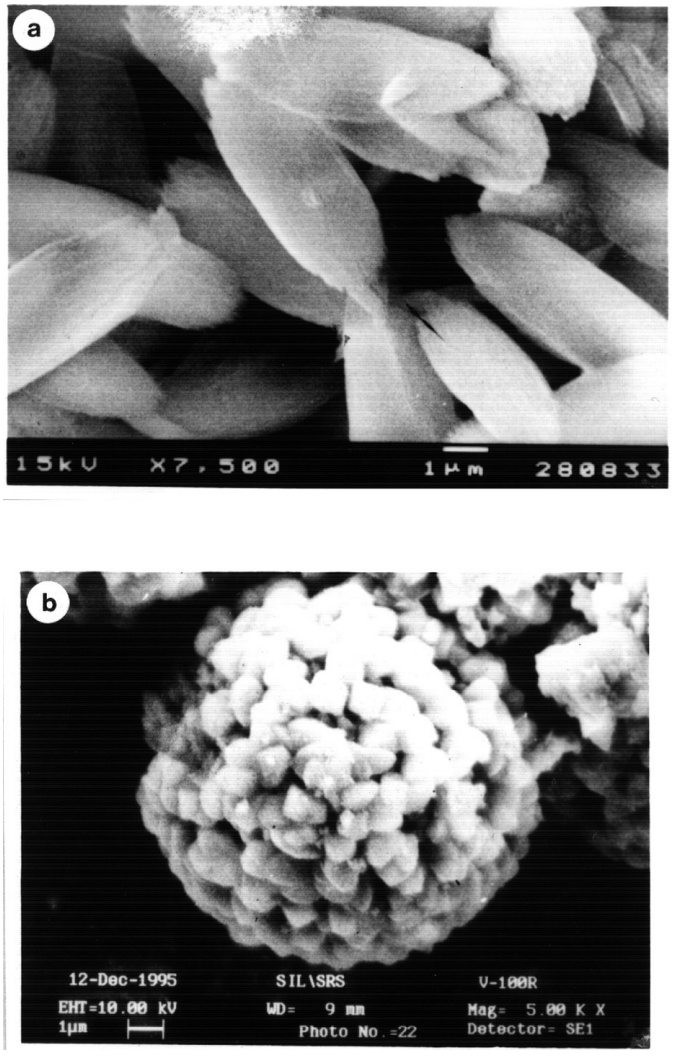

FIG. 2. Scanning electron micrographs of Sil-2 (a) and Zr-Sil-2 sample with Si/Zr = 100 (b).

spectra and attributed this vibration to the possible formation of Si–O–Zr linkages in their samples.

The diffuse reflectance (UV-visible) spectrum of Zr-Sil-2 (100) sample (Fig. 4, curve c) shows a characteristic absorption at about 210 nm attributable to a charge transfer (CT) character involving the Zr (IV) (tetrahedral configuration) sites (8). This absorption is absent in the spectra of amorphous Zr-silica and Zr-impregnated Sil-2 samples (curves a and b, respectively). These electronic transitions are clearly distinguishable from those in pure ZrO_2 (monoclinic symmetry) which shows strong absorption at about 240 and 310 nm (Fig. 5, curve d). The N_2 adsorption isotherms of Zr-Sil-2 samples are characteristic of microporous materials. The micropore areas are in the range of 385–481 m^2g^{-1} in comparison to a value of 301 $m^2 g^{-1}$ obtained for Sil-2 (Table 1). The amounts of water, *n*-hexane and cyclohexane probe molecules adsorbed on the

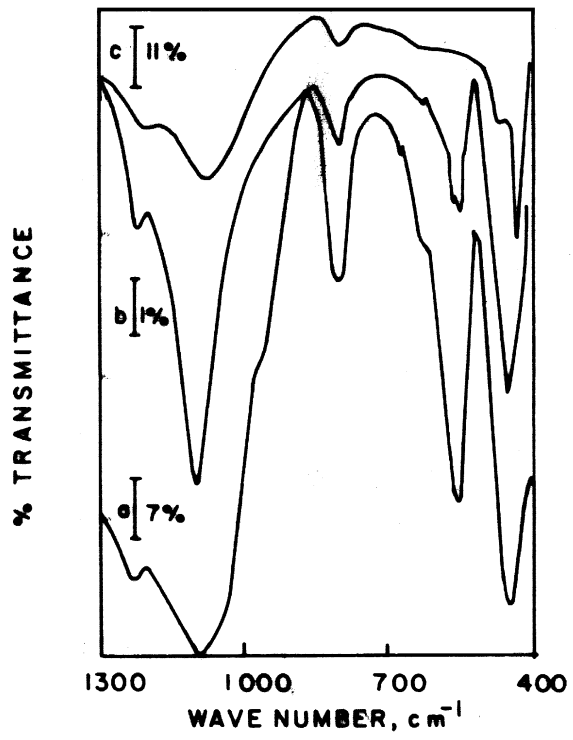

FIG. 3. Framework FT-IR spectra of Zr-Sil-2, Zr-impregnated Sil-2, and amorphous Zr-silica samples (curves a to c, respectively).

samples are compared to that by pure Sil-2 (Table 1). The sorption capacities of Zr silicates indicate the absence of any pore blockage due to occluded or amorphous material in the microporous structure.

In Fig. 5, the infrared spectrum of pyridine (py) adsorbed on Sil-2 (curve a) is compared with those of Zr-Sil-2 samples

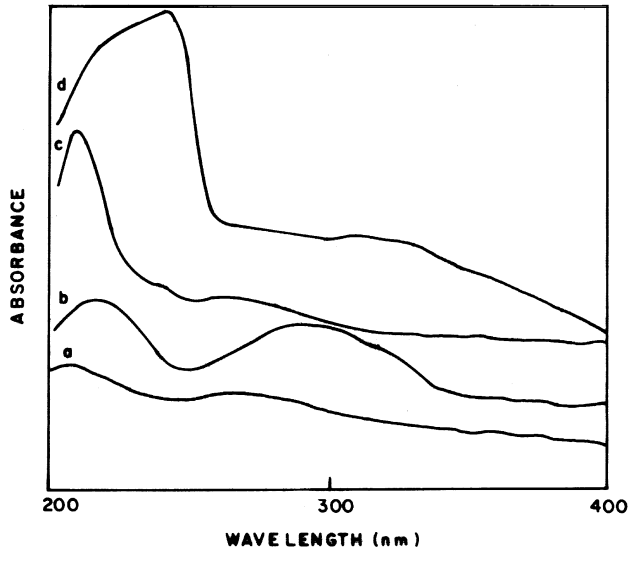

FIG. 4. DR UV-visible spectra of amorphous Zr-silica (curve a), Zr-impregnated silica (b), Zr-Sil-2 (c), and pure ZrO_2 samples (d).

TABLE 1

Physico-Chemical Properties of Zr-Sil-2 Samples

Sample	Si/Zr[a]	Zr per uc[b]	V_{uc} (Å^3)	Sorption capacities (wt%)[c]			Micropore area[d] $m^2\ g^{-1}$	Micropore vol. mL g^{-1}	Mesopore area $m^2\ g^{-1}$
				Water	Cyclohexane	*n*-Hexane			
Silicalite-2	—	—	5341	7.4	7.0	12.5	301	0.12	*
Zr-Sil-2 (300)[e]	345	0.28	5361	7.9	9.0	13.3	460	0.13	*
Zr-Sil-2 (200)	191	0.50	5363	8.0	8.7	13.6	481	0.14	*
Zr-Sil-2 (100)	102	0.94	5375	8.2	9.5	14.0	400	0.12	54
Zr-Sil-2 (65)	61	1.57	5347	7.6	9.0	13.2	385	0.13	65

[a] Si/Zr molar output ratio determined by EDX.
[b] Total amount (molar output of Zr) in the product per unit cell = (Total number of "T" sites ÷ (Si/Zr)).
[c] Gravimetric adsorption at $p/p_o = 0.5$ and at 298 K.
[d] Volumetric adsorption at $p/p_o = 0.05$ and at 77 K.
[e] Si/Zr molar input ratio of the gel in parentheses.
*Negligible.

with Si/Zr molar ratios of 100, 200, and 300 (curves b, c, and d, respectively) after evacuation at 348, 383, and 473 K. The spectra of the Zr-Sil-2 samples show strong bands at 1620 and 1450 cm^{-1} due to the py coordinately bound to Lewis acid sites (V_s modes) (17). A weak band at 1545 cm^{-1} is assigned to the pyridinium ion which is absent in the spectrum of Sil-2. These weak Brønsted acid sites may be due to the interaction between py chemisorbed on Lewis acid sites and a nearby surface OH group (18). However, the desorption of py at increasing temperature (>473 K) resulted in preferential removal of Brønsted bound py relative to Lewis-bound py. A band at 1490 cm^{-1}, due both to the coordinated py and py chemisorbed on protonic acid sites (i.e., pyridinium ion), is also observed (19). It is observed that Sil-2 sample has no coordination sites at increasing temperature to interact with gaseous pyridine. Therefore, Zr-Sil-2 appears to be more acidic than Sil-2. The $Si{-}O^{\delta-}\ldots Zr^{\delta+}$ bridges, because of their strong polarization, may be the preferable sites for the adsorption of polar molecules. These IR results could be interpreted as an indication that the tetrahedral Zr in the silicalite lattice bears a δ^+ charge so that the O...Zr bond may be viewed as a Lewis acid–base pair. A similar interpretation has been given for the origin of Lewis acid sites in titanium silicalites (20).

Hydroxylation of phenol over Zr-Sil-2 samples were carried out using aqueous H_2O_2 (30 wt%) as an oxidizing agent. The Zr-Sil-2 (100) sample showed 25.4% H_2O_2 selectivity with turnover number (mole of phenol converted per mole of Zr atom) of 71.0 (Table 2). In the product distribution, a catechol (CAT) to hydroquinone (HQ) ratio of 0.94 for the Zr-Sil-2 (100) sample indicates a certain degree of product shape selectivity. A CAT/HQ ratio of 0.9 to 1.3 has been reported for titanium and vanadium silicate molecular sieves (TS-2 and VS-2) (21) which are crystalline (MEL-type) and microporous and are similar to Zr-Sil-2 in their properties, having Ti or V in framework positions. These results indicate that in addition to being well dispersed, the Zr^{4+} ions are located within the channels of MEL structure as active sites. In order to check the catalytic behavior of Zr-Sil-2, the hydroxylation runs were carried out on Zr-impregnated Sil-2, amorphous Zr-silica sample and Zr-free Sil-2 samples under identical conditions and these were found to have negligible activity in this reaction (Table 2). Apparently only isolated zirconium ions, which are present in the framework of silicalite-2, are active in the reaction. The catalytic activity, as well as the selectivity for the products (catechol (CAT) and hydroquinone (HQ)), is comparable to those of Zr-Sil-1 which showed 34.0% H_2O_2 selectivity (turnover number = 112) with CAT/HQ ratio of 1.4 (9). Although the catalyst can be reused (with marginal loss in activity) after filtration and washing with acetone to remove tar, the original catalytic activity of Zr-Sil-2 can be restored after calcination in air at 773 K for 6–8 h.

TABLE 2

Hydroxylation of Phenol[a]

Catalyst	TON[b]	H_2O_2 sel.[c]	Product distribution (wt%)			
			PBQ	CAT	HQ	Tar[d]
Zr-Sil-2(100)	71.0	25.4	1.3	41.9	44.6	12.2
Zr/Sil-2[e]	—	3.0	38.5	58.2	3.3	*
Amorphous Zr-silica	—	2.4	35.5	62.6	1.9	*
Sil-2	—	4.4	58.4	41.4	0.2	*

[a] Reaction conditions: catalyst = 0.5 g; solvent (water) = 10 g; phenol/H_2O_2 (mol) = 3; reaction duration = 10 h; temperature = 353 K.
[b] Turnover number = mole of phenol converted per mole of Zr atom.
[c] H_2O_2 utilized for the formation of parabenzoquinone (PBQ), catechol (CAT), and hydroquinone (HQ), excluding tar.
[d] High boiling fractions (>573 K) estimated from the TG analysis in the products.
[e] Zr-impregnated Sil-2, for similar amount of Zr as in the case of Zr-Sil-2 (100).
* Negligible.

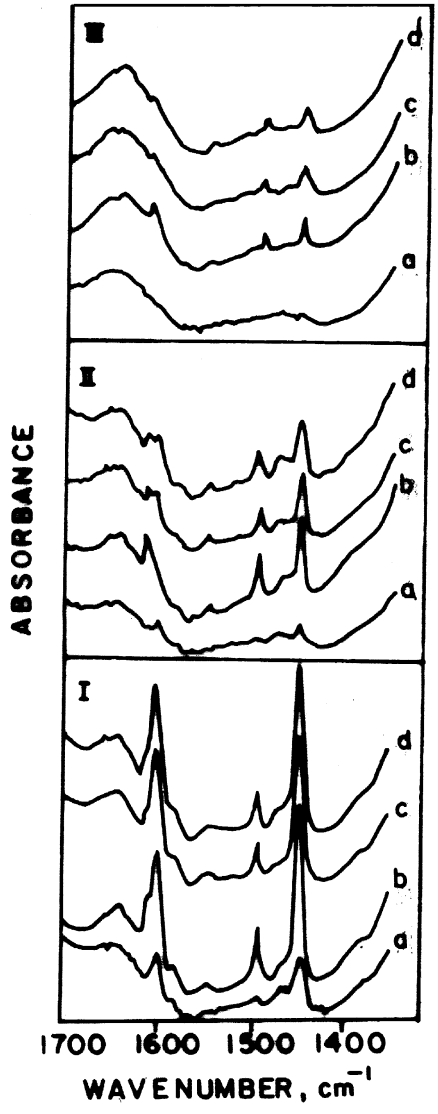

FIG. 5. Infrared spectra of pyridine adsorbed on Sil-2 sample (curve a) and Zr-Sil-2 samples with Si/Zr molar ratios of 100, 200, and 300 (curves b to d, respectively) after evacuation at (I) 346 K, (II) 383 K, and (III) 473 K.

An increase in unit cell volume (from 5341 to 5375 $Å^3$) corresponding to the theoretical expansion due to the larger size of Zr^{4+} ions, the formation of Si–O–Zr linkages (FTIR spectra), and the characteristic charge transfer transition in the Td configuration (DR UV-visible spectra) indicate that up to 1.0 Zr atom per unit cell is substituted isomorphously in the framework positions of Zr-silicate in the MEL structure. This is further supported by the catalytic activity data in the hydroxylation of phenol and the CAT/HQ ratio of about 0.94 in the products. The pyridine adsorption studies showed the presence of strong Lewis acid sites and weak Brønsted acid sites on the surface of Zr-silicate samples.

ACKNOWLEDGMENTS

We acknowledge the help extended by Dr. S. R. Sainkar (SEM), Mrs. N. E. Jacob (TGA),and Dr. D. Chakraborty (ICP analysis). B.R. thanks DST, New Delhi, for a project assistantship. We are very grateful to Professor S. Kaliaguine, University of Laval, Quebec, Canada for the IR spectra of adsorbed pyridine samples.

REFERENCES

1. Bellussi, G., Carati, A., Clerici, M. G., Esposito, A., Millini, R., and Buonomo, F., Belg. Patent 1,001,038 (1989).
2. Reddy, J. S., Kumar, R., and Ratnasamy, P., *Appl. Catal.* **58**, L1 (1990).
3. Mal, N. K., Ramaswamy, V., Ganapathy, S., and Ramaswamy, A. V., *Appl. Catal. A: General* **125**, 233 (1995).
4. Herbert, B., Heinz, L., Ernst Ingo, L., and Friedrich, W., E.P. 77,523 A2 (1983).
5. Costantini, M., Guth, J. L., Lopez, A., and Popa, J. M., E.P. 466,545 A1 (1991).
6. Dongare, M. K., Singh, P., Moghe, P., and Ratnasamy, P., *Zeolites* **11**, 690 (1991).
7. Fricke, R., Kosslick, H., Tuan, V. A., Grohmann, I., Pilz, W., Storek, W., and Walther, G., *Stud. Surf. Sci. Catal.* **83**, 57 (1994).
8. Wang, G. R., Wang, X. Q., Wang, X. S., and Yu, S. X., *Stud. Surf. Sci. Catal.* **83**, 67 (1994).
9. Rakshe, B., Ramaswamy, V., Vetrivel, R., and Ramaswamy, A. V., *Catal. Lett.*, submitted.
10. Kokotailo, G. T., Chu, P., Lawton, S. L., and Meier, W. M., *Nature* **275**, 119 (1995).
11. Dirken, P. J., Smith, M. E., and Whitfield, H. J., *J. Phys. Chem.* **99**, 395 (1995).
12. Scarano, D., Zeechina, A., Bordiga, S., Geobaldo, F., Spoto, G., Petrini, G., Leofanti, G., Padovan, M., and Tozzola, G., *J. Phys. Chem.* **89**, 4123 (1993).
13. Bellussi, G., Carati, A., Maddinvelli, M. G., and Millini, R., *J. Catal.* **133**, 220 (1992).
14. Liu, Z., and Davis, R. L., *J. Phys. Chem.* **98**, 1253 (1994).
15. Sohn, J. R., Jang, H. J., Park, E. H., and Park, S. E., *J. Mol. Catal.* **93**, 149 (1994).
16. Dang, Z., Anderson, B. G., Amenomiya, Y., and Morrow, B. A., *J. Phys. Chem.* **99**, 14437 (1995).
17. Morterra, C., and Cerrato, G., *Langmuir* **6**, 1810 (1990).
18. Basila, M. R., Kantner, T. R., and Rhee, K. H., *J. Phys. Chem.* **68**, 3197 (1964).
19. Ebitani, K., Hattori, H., and Tanabe, K., *Langmuir* **6**, 1743 (1990).
20. Bittar, A., Adnot, A., Sayari, A., and Kaliaguine, S., *Res. Chem. Intermediates* **18**, 49 (1992).
21. Ramaswamy, A. V., and Sivasanker, S., *Catal. Lett.* **22**, 239 (1993).

Bhavana Rakshe
Veda Ramaswamy
A. V. Ramaswamy[1]

Catalysis Division
National Chemical Laboratory
Pune-411 008, India

Received February 28, 1996; revised June 27, 1996; accepted July 15, 1996

[1] To whom correspondence should be addressed. E-mail: avr@ncl.ernet.in; Fax: 91-212-334761